

PAPER VI

**Short timescale inkjet ink
component diffusion**

**An active part of the absorption mechanism into
inkjet coatings**

In: Journal of Colloid and Interface Science
2012(365)1, pp. 222–235.

Copyright 2011 American Chemical Society.
Reprinted with permission from American
Chemical Society.



Short timescale inkjet ink component diffusion: An active part of the absorption mechanism into inkjet coatings

T.T. Lamminmäki^{a,*}, J.P. Kettle^{a,1}, P.J.T. Puukko^{a,1}, C.J. Ridgway^c, P.A.C. Gane^{b,c}

^a VTT Technical Research Centre of Finland, P.O. Box 1000, 02044 VTT, Finland

^b Aalto University, School of Science and Technology, Faculty of Chemistry and Materials Sciences, Department of Forest Products Technology, P.O. Box 16300, FIN-00076 Aalto, Finland

^c Omya Development AG, CH-4665 Oftringen, Switzerland

ARTICLE INFO

Article history:

Received 22 December 2010

Accepted 19 August 2011

Available online 28 August 2011

Keywords:

Diffusion

Absorption

Porosity

Permeability

Ink dye adsorption

Inkjet printing

Coating

ABSTRACT

The structures of inkjet coatings commonly contain a high concentration of fine diameter pores together with a large pore volume capacity. To clarify the interactive role of the porous structure and the coincidentally occurring swelling of binder during inkjet ink vehicle imbibition, coating structures were studied in respect to their absorption behaviour for polar and non-polar liquid. The absorption measurement was performed using compressed pigment tablets, based on a range of pigment types and surface charge polarity, containing either polyvinyl alcohol (PVOH) or styrene acrylic latex (SA) as the binder, by recording the liquid uptake with a microbalance. The results indicate that, at the beginning of liquid uptake, at times less than 2 s, the small pores play the dominant role with respect to the inkjet ink vehicle imbibition. Simultaneously, water molecules diffuse into and within the hydrophilic PVOH binder causing binder swelling, which diminishes the number of active small pores and reduces the diameter of remaining pores, thus slowing the capillary flow as a function of time. The SA latex does not absorb the vehicle, and therefore the dominating phenomenon is then capillary absorption. However, the diffusion coefficient of the water vapour across separately prepared PVOH and SA latex films seems to be quite similar. In the PVOH, the polar liquid diffuses into the polymer network, whereas in the SA latex the hydrophobic nature prevents the diffusion into the polymer matrix and there exists surface diffusion. At longer timescale, permeation flow into the porous coating dominates as the resistive term controlling the capillary driven liquid imbibition rate.

© 2011 Elsevier Inc. All rights reserved.

1. Introduction

In inkjet printing, the ink transfer, meaning the delivery, spreading and penetration of an ink droplet on and into the substrate surface is the most important property that is reflected in the final print quality. During the inkjet printing process, there is no physical contact between the ink nozzles and paper surface, contrary to the case of conventional printing nips, and therefore the importance of the dynamics of free ink transfer onto the surface is emphasized in inkjet printing. Currently there are two main types of drop delivery systems: drop-on-demand (DOD) and continuous jetting (CJ). In DOD, only those droplets are produced, which are intended to arrive on the printing surface, whilst in CJ, there is a stream of droplets produced at high frequency, from which most of the droplets are deflected away and only a few of them reach the substrate

surface. In the CJ inkjet, a piezo crystal causes a pressure change in the nozzle and the ejection of ink out of the nozzle. In the DOD method, there are several different droplet formation techniques used, but the most common are piezoelectric and thermal.

As the droplet has formed during the flight between nozzle and printing surface it arrives finally at the substrate surface with a given impact related to the inertia of the droplet mass arriving at the defined velocity, which delivers a lower force than those associated with traditional printing press nips. There are many studies concerned with droplet impact and settling onto substrate surfaces [1–9]. Two theoretical approaches are considered to dominate when describing fluid spreading on a porous surface during droplet impact – the hydrodynamic model [3,6,10–12] and a molecular kinetic model [13,14]. These models have been frequently combined [15,16]. The droplet formation and flight dynamics have been studied, for example, by the working groups of Eggers and Villermaux [8] and Basaran [4,5] and the effect of the impact of the droplet onto the surfaces by Lembach et al. [9] and Reznik et al. [3]. The mass-related forces are related to the motion of the inkjet ink droplet, for example when it undergoes acceleration (usually in the form of deceleration). The Bond

* Corresponding author. Fax: +358 20 722 7026.

E-mail addresses: taina.lamminmaki@vtt.fi (T.T. Lamminmäki), john.kettle@vtt.fi (J.P. Kettle), pasi.puukko@vtt.fi (P.J.T. Puukko), cathy.ridgway@omya.com (C.J. Ridgway), patrick.gane@tkk.fi, patrick.gane@omya.com (P.A.C. Gane).

¹ Fax: +358 20 722 7026.

number describes the relationship between the droplet response to acceleration and surface tension. A low Bond number indicates that surface tension dominates over the impact process. As the droplet strikes the substrate, the connection between the kinetic energy flow and surface tension of liquid is described by the Weber number. If the Weber number is high, it indicates that the kinetic energy dominates at the droplet striking and liquid thin film flowing. In the practical case, for example in a Versamark® VX5000e inkjet printing press, where the droplet strikes the surface with a fairly high kinetic energy, the droplet can arrive onto the paper surface with the speed of 15 m s^{-2} . Under these conditions, the ink spreading is dominated by inertia.

The commonly used aqueous-based dyes or pigment inks should lose their liquid diluent at an adequate speed into the substrate surface structure so that the various ink colours cannot mix together and exhibit intercolour bleeding. On the other hand, the ink amount is usually greater than in the case of traditional offset or gravure printing, and therefore the substrate surface should contain adequate pore volume to accommodate the entire applied ink vehicle (meaning the solvent water and the soluble chemical compounds in the inkjet ink) into the structure.

The fluid movement in a saturated structure is commonly stated to comply with the Navier–Stokes equation, from which, in the case of low viscosity inkjet ink, once again it can be derived that the most important properties of the ink are represented by surface tension, viscosity and specific gravity of the fluid [3,7,12]. The theory of fluid movement in the pores is thus based on the balance between viscous drag and the wetting force, commonly expressed in the form of the Lucas–Washburn equation [17]. Most work in the previous literature relates to the loss of liquid from saturated pore structures, usually during the drying process, for example the modelling description of Brethour and Scriven [18] who also consider convection as a potential mechanism during drying. The absorption phenomenon into nanostructures of a few molecular dimensions in thickness has been studied by Gerung et al. [19,20]. Conversely, studies of liquid absorption are generally observational, and provide either interpretation of equilibrium absorption [13] or qualitative deviation from Lucas–Washburn [21]. Without resorting to molecular dynamics, short timescale phenomena occurring during the initial absorption phase need to be considered outside the equilibrium phenomena described typically in the Lucas–Washburn force balance. These can be captured by considering the role of droplet impact inertia in initiating the top surface void filling and subsurface structure by liquid, followed by the action of nanopores in defining the liquid uptake as bulk inertial drag retards uptake into the deeper-lying larger pores. This has been described and modelled by Schoelkopf et al. [15] and Ridgway and Gane [22], who apply the Bosanquet equation [23] to highlight the role of pore size differentiation prior to the onset of viscous drag equilibrium. It is shown that the finest pores drive the initial capillary filling at the wetting front [22].

Besides the requirements of absorption during the very fast short timescale phenomena of initial ink uptake, the ink colourant should bind to the top part of the substrate to develop a high print density and good rub-off resistance and water fastness. As the inkjet ink penetrates into the porous substrate, and particularly in the case of coated media, i.e. the coating layer structure, a variety of interaction phenomena influence where the ink vehicle and colourant molecules penetrate and finally become distributed. At first, the arrived ink should wet the surfaces of pigment and binders forming the surface void structures leading to capillary flow by internal pore wetting into the bulk of the coating pore network structure, during which there is a separation of the ink components, via mechanisms including adsorption, diffusional movement, polymerisation (if there exist polymerisable components) and during drying of the ink and coating [24].

The main interest in the work reported here is concentrated on the diffusional movement which happens already at the capillary flow boundary between the liquid and surface interface, but in the prior literature is generally assumed to be a quite small effect in volume terms [2], even though the vapour diffusion at the interface is frequently implicated in defining the advancing contact angle [25]. The significance of diffusion of ink components into such structures as polymer layers is usually assumed to increase during time, when the ink has penetrated deeper into the structure. These assumptions were derived from studies of generally homogeneously distributed pores. Modern inkjet coatings, however, consist of a collection of individual porous particles, for example modified calcium carbonate, which, when packed together in the coating, generate a discretely bimodal pore size distribution [26–28]. The bimodality is related to the combination of high capillarity internal pores and the permeability-controlling inter-particle pores. The role of diffusion into soluble binders, which can fill or partially fill the accessible intra-particle pores, and thus occurring at the beginning of the inkjet ink setting process, has not been studied so widely.

During the diffusion of inkjet ink molecules, ink vehicle as well as the colourant molecules migrate from a region of high concentration to a region of lower concentration by Brownian motion [29]. The driving force is maintained in this phenomenon by the gradient of concentration. There exists many different types of diffusional movement, but probably the most important, with respect to inkjet inks, are described by [29–31] as:

- Bulk diffusion, which means general motion of the inter-skeletal (region between the solid particles of the porous matrix) bulk molecules of the liquid or gas within the coating/deposited layer.
- Surface diffusion, where the motion of atoms, molecules and atomic clusters follows the surfaces of material.
- Knudsen diffusion, when the diffusivity is determined by the size of capillaries instead of the solvents or solutes alone (Fig. 1).
- Osmosis, defined as the spontaneous net movement of water across a semi-permeable membrane from a region of low solute concentration to a region with a high solute concentration, down a water concentration gradient, or, as more usually described, up a solute concentration gradient. It is a physical process in which a solvent moves, without input of external energy.

The external pressure, temperature, moisture content and uniformity of the materials define which diffusion mechanism dominates in the absorption and/or adsorption of water molecules [29,32]. There are only a few studies which support the idea of diffusional movement at short timescale of inkjet ink during imbibition [27,33,34]. Resulting surface and just-subsurface flow during the inertially-driven drop impact affects the establishment of wetting, i.e. overcomes any likelihood of top surface wetting delay.

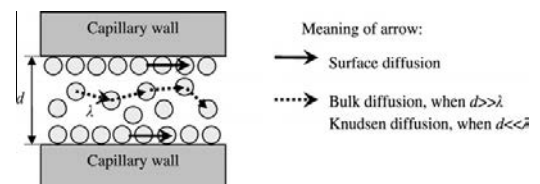


Fig. 1. Diffusion types in the inkjet ink transfer. d is pore diameter and λ distance between atoms, molecules, or atomic clusters (mean free path).

This is followed by absorption into the nanopores, which is expected to account for the filling of the finest internal structure elements [26] acting with a linear proportionality to time. The establishment of longer time viscous limited capillary flow is manifested by a square root of time proportionality.

The objective of this work is to clarify the role of liquid polarity (ink vehicle polarity) upon the sorption and diffusion of vehicle into different coating pigment containing structures combined with either a hydrophilic, swelling polyvinyl alcohol (PVOH), or an internally hydrophobic, non-swelling styrene acrylic latex (SA). Throughout, the imbibition of ink is progressively limited by the prerequisite of diffusion-controlled wetting, either of the polymer filled nanopores (PVOH) or of the polymer surface film on the pigments (PVOH or SA latex). Model coatings are studied based on comparing a standard anionically dispersed ground calcium carbonate (GCC) and two calcium carbonate-based inkjet coating pigment technologies, one based on modified calcium carbonate (MCC, displaying a discretely bimodal pore size distribution) and the other based on precipitated calcium carbonate (PCC). PVOH is used as the example of a “diffusion driving” (water diffusive) binder and is compared with an SA latex considered as a binder being internally non-diffusive to water.

A comparison of water moisture diffusion into and on films made from the two binder types allows a comparison to be drawn in respect to their diffusion capacity rates. The concentration gradient of liquid water rather than vapour is shown to enhance the volume diffusion uptake even further.

2. Materials and methods

2.1. Raw materials

The idea was to use coating pigments which provide different coating layer structures: one with large pores versus one with small pores and the third structure having both small and large pores distributed with discrete bimodality. The pigments were modified calcium carbonate (MCC, Omyajet B6606²), ground calcium carbonate (GCC, Hydrocarb 90²) and precipitated calcium carbonate (PCC, JetCoat 30³). The properties of the pigments are introduced in Table 1. MCC and GCC were provided as dry powders. The GCC was derived from Turkish marble, in dispersant-free form. The moisture and water equilibrium in suspension provides the cationic starting point in respect to zeta potential, i.e. adsorbed CaOH⁺ ion (cationic) in equilibrium with the dissolution of Ca²⁺ and OH⁻. This is then very quickly translated by the adsorption of polyacrylate via the calcium neutralisation and coagulation effect to the anionic form, as Eriksson et al. [35] have shown. The PCC, on the other hand, was supplied in pre-dispersed slurry form. Using image analysis particle tracking during Brownian motion (NanoSight⁴) it could be shown that the PCC pigment contained two distinct particle sizes. The smaller diameter (20–30 nm) particles were the primary particles, whereas the larger particles, located in the area of 260–300 nm, consisted of agglomerates of the finer primary ones. The two distributions together gave an average particle size of 250 nm.

Two contrasting binders were used: a non-ionic polyvinyl alcohol (PVOH, Mowiol 40–88⁵) and an anionically stabilized styrene acrylate latex (SA, CSA 212⁶). The PVOH had a degree of hydrolysis of 87.7 ± 1.0%. The latex had a particle size of 180 nm and a glass

transition temperature of –20 °C. An anionic sodium polyacrylate (Polysalz S⁶, molecular weight 4000 gmol⁻¹) and a cationic poly(diallyl dimethyl ammonium chloride) (polyDADMAC, Cartafix VXU⁷) were used as dispersing and charge modifying agents, respectively. In the pigment particle dispersing, the dispersing agent amount was 0.5 pph (parts by weight of binder per 100 parts of pigment). In Table 2, the pigments, in their final water suspended form, are described in formulations both prior to and after the addition of binder. The binder content was 1 or 7 pph (Table 2). Though not all the coating colours were measured in respect to zeta potential, the colours were anionic except the originally cationically dispersed MCC, and the coatings with SA latex provided a higher anionicity than the PVOH containing coating colours.

2.2. Testing methods

The coating tablets were produced from coating colours by a wet filtration system [26,36] under the external pressure 20 bar. The tables were dried at 60 °C over night. The PVOH uniformity within the tablets was studied with a Thermo Nicolet Nexus 870 FT-IR spectrometer⁸ (IR spectra from KBr-tablets, Fig. 2). The actual amount of PVOH was not calculated from the results of the IR spectra, only the IR spectra difference between the sides of the tablet was detected. The results show that the wire filter side (lower surface) of the tablet had a higher concentration of PVOH. (For this difference measurement, the PVOH content was 0.7 pph, whereas, in our microbalance study, the binder amount used was slightly higher, 1 pph.) Therefore, the final tablets fashioned for the microbalance absorption analysis were prepared so that both sides of the tablet (top and bottom side) were tested and an average formed, each having the same time in contact with the liquid. The filtrate that formed during the tablet making procedure was also analyzed with FT-IR spectrophotometry, and the result showed that it also contained PVOH, confirming the soluble nature of the binder.

The polarity of the liquid, and its effect on imbibition into pigment tablets, was studied using distilled water (100% polar) and hexadecane (100% apolar), respectively (Table 3). The edges of the formed samples were polished and covered with octamethyl trisiloxane/toluene⁹ so that the pores of edge areas did not affect the liquid uptake by exterior planar wetting. The uptake of the liquid was measured gravimetrically with an automated microbalance [36–38]. The temperature of surrounding air was 23.0 ± 1.5 °C. The weight loss due to the water evaporation during the measurement was taken into account in the results. Hexadecane has a minimal evaporation over this time period.

The porosities of the coating layers were determined by a silicon oil absorption saturation method as well as the microbalance analysis by water and hexadecane at equilibrium saturation. In the silicon oil measurement, the pigmented tablet was left for 1 h in the oil, and the weight of tablet before and after oil saturation was measured. For all liquids, the absorbed liquid volume was measured as the weight change between the “dry” and saturated sample divided by the density of the respective liquid. The porosity of the sample for each liquid was thus defined as the volume of absorbed liquid at saturation divided by total volume of sample. All determinations were made at room temperature (23 ± 2 °C) and normal atmospheric pressure.

The pore size distribution was analyzed by mercury porosimetry (Micrometrics AutoPore IV¹⁰). The coating structure was impregnated with mercury using both low and high pressures. The

² Omya AG, Postfach 32, CH-4665 Oftringen, Switzerland.

³ Minerals Technologies Europe, Ikaros Business Park, Ikaroslaan 17, Box 27, 1930 Zaventem.

⁴ NanoSight Ltd., Minton Park, London Road, Amesbury, Wiltshire SP4 7RT, UK.

⁵ Kuraray Specialities Europe GmbH, Building D 581 D-65926, Frankfurt am Main, Germany.

⁶ BASF Aktiengesellschaft, Paper Chemicals, 67056 Ludwigshafen, Germany.

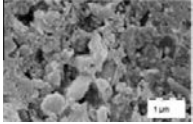
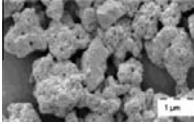
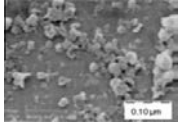
⁷ Clariant International AG, Rothausstrasse 61, CH-4132 Muttenz 1, Switzerland.

⁸ Thermo Nicolet, 5225 Verona Road, Madison, WI 53711-4495, USA.

⁹ Dow Corning GmbH, Postfach 13 03 32, 65201 Wiesbaden, Germany.

¹⁰ Micrometrics Instrument Corporation, 4536 Communications Drive, Norcross, GA 30093, USA.

Table 1
The properties of coating pigment.

Pigment property	Ground calcium carbonate (GCC) [35]	Modified calcium carbonate (MCC)	Precipitated calcium carbonate (PCC)
Weight median diameter of particle ($d_{50w/w}$) (μm)	1.10	2.70	Small fraction 0.02–0.03 Ave. 0.25*
Specific surface area (BET, ISO 9277) ($\text{m}^2 \text{g}^{-1}$)	8.5	46.2	73.9
Product form	41.7 (without added dispersant) and –40.2 mV (added sodium polyacrylate)	Powder (cationically pre-dispersed)	Anionic slurry
SEM picture			

* NanoSight (results had two peaks: small fraction at 0.02–0.03 μm and average at 0.25 μm).

porosity and pore size distribution were calculated adopting the Pore-Comp¹¹ correction, which takes account of penetrometer expansion, mercury compression and compression of the sample skeletal material, expressed as the elastic bulk modulus, according to Gane et al. [41].

Binder films were produced in order to establish the moisture uptake associated with the binder alone. PVOH was formed into a film using a Teflon^{®12} mould and dried at 23 ± 2 °C. The thickness of the partially hydrolysed PVOH film was 225 μm . A latex film formed from the SA binder was made to a thickness of 284 μm using an Erichsen¹³ film applicator (Model 288) followed by drying in an oven at 105 °C for 5 min. The diffusion coefficient for water into the binder films, was calculated also from the results of the microbalance showing weight change as a function of the moisture content of the surrounding air in the balance chamber. The moisture content was adjusted step by step starting from 0.1% RH and progressing to 5%, 50%, 93% RH and finally to 50% RH. The temperature of the measuring chamber was controlled to be at 23.5 ± 0.3 °C.

3. Results

3.1. The coating layer structures

The porosities of the coating layers are shown in Fig. 3: the coating made from the normal offset standard GCC had the lowest porosity, and the coating of the dual-pore size MCC and inkjet speciality PCC the highest. In the case of MCC, the addition of SA latex produced a coating layer structure that had slightly higher pore volume than when using the same amount of polyvinyl alcohol. The cationic dispersing of the MCC pigment seems to produce a slightly higher porosity than the subsequent anionic re-dispersing (no binder), suggesting either a slight flocculation remains in the cationic state or that the additional polymer itself reduces pore volume. With GCC and PCC pigments, SA latex addition gave a lower pore volume than when adding PVOH. The results from different measurements had some differences, especially when the results of non-pressurized measurements (saturation by imbibition) are compared to the results of mercury porosimetry (pressurized).

The pore size distributions of the coatings diverged a lot (Fig. 4A–C), thus enabling the effect of pore structure to be studied in detail. The PCC pigment coating produced the smallest pore diameters, which were in the area of 15–60 nm. The pores of the GCC pigment structure located in the area of 90–330 nm, and

MCC had a dual-pore size distribution, where the pore diameters located in the area of 20–60 nm (intra-particle) and 300–700 nm (inter-particle). The addition of PVOH binder decreased the inter-particle pores of MCC coatings to 200–400 nm and SA latex addition increased it to 500–1000 nm. In the case of GCC, all pore size distributions were very similar since the amount of binder added was confined to 1 pph.

3.2. The transport of polar and non-polar liquid

Fig. 5A illustrates, as an example, the absorbed water or hexadecane volume per initial tablet–liquid contact area against time for the coating tablet structures during the microbalance measurements. In the beginning of the absorption, the liquids absorbed very quickly into the coating layer. Then there was a region of slower increase and finally the uptake stopped due to the saturation. A closer study of the absorption results (Fig. 5B) shows that there exist two increasing regions in the absorption curve in the case of MCC with just 1 pph of PVOH, both of which have a linear correlation with square root of time. All the coatings had a linear proportionality to \sqrt{t} over a ~ 2 s timescale. The domination of different sorption phenomena in the coating structure varies during time. Therefore, it can be assumed that before ~ 2 s the capillary wetting and surface diffusion dominate, and after that it turns toward a domination of permeation resistance acting to equilibrate against the capillary wetting and bulk diffusion forces. In a high-speed inkjet printing press, such as the Versamark[®] VX5000e, the delay between the first printing nozzle and the beginning of the dryer is 17 s at a web speed of 15 m min^{-1} and at 100 m min^{-1} , 2.6 s. Therefore, it can be concluded that the times considered here, and the transition of phenomena between them, are highly relevant when considering inkjet printing. The MCC coating with 7 pph SA had only a slight change in the slope of curve with \sqrt{t} (Fig. 5D), reflecting the reduced permeability of this coating as shown by the lower specific pore volume associated with the larger pore size in the discrete bimodal distribution (Fig. 4). Furthermore, if we look at the data over the longer time scale (Fig. 5C), this sample containing the higher level of latex shows a further time-dependent variation of the water absorption rate. This accelerated response over time probably relates further to the action of latex-associated surfactant.

The absorption rate of short and long timescale during the liquid uptake can be expressed [15,42] as

$$\frac{d(V(t)/A)}{d\sqrt{t}} = \frac{d((m(t)/\rho)/A)}{d\sqrt{t}} \quad (1)$$

where $V(t)$ is the volume of uptaken liquid at the time t , A the cross-section area of tablet, $m(t)$ is the mass uptake of the liquid and ρ the

¹¹ Pore-Comp are a software network model and sample compression correction software, respectively, developed by the Environmental and Fluid Modelling Group, University of Plymouth, PL4 8AA, UK.

¹² Polytetrafluoroethylene, Du Pont.

¹³ Erichsen GmbH & Co., Am Iserbach 14, D-58675 Hemer, Germany.

Table 2
The formulation of the coating colours.

Coating (pph)	Cationic MCC	Anionic MCC	Anionic MCC + 1 pph PVOH	Anionic MCC + 1 pph SA	Anionic MCC + 7 pph PVOH	Anionic MCC + 7 pph SA	Anionic GCC	Anionic GCC + 1 pph PVOH	Anionic GCC + 1 pph SA	PCC ^a	Anionic PCC + 1 pph PVOH	Anionic PCC + 1 pph SA
Pigment												
MCC	100	100	100	100	100	100	100	100	100	100	100	100
GCC												
PCC												
Dispersing agent												
Anionic sodium polyacrylate		0.5	0.5	0.5	0.5	0.5	0.5	0.5	0.5	N/A	N/A	N/A
Cationic polyDADMAC	0.5	No	1	7	7	No	No	1	No	No	1	
Binder												
PVOH (partially hydrolysed)												
SA latex												
Zeta-potential (AcoustoSizer II ^b), mV												
	23.6	-36.7	N/A	1	-11.9	7	-9.0	N/A	1	N/A	-3.1	1
				N/A		-37.0		N/A	N/A			N/A

^a PCC pigment was provided by the manufacturer as a slurry-form; exact type and amount of dispersing agent are not known.

^b AcoustoSizer II is a product name of Colloidal Dynamics/Agilent, Technologies (Finland Oy), Linnitustie 2B, FI-02600, Espoo, Finland.

density of liquid. The absorption rate is recorded as a linear trend line from the gradient of the volume per contact area of sample against the square root of time. We separated the short timescale (under 2 s) and the long timescale absorption for all the pigment and binder combinations (Figs. 6 and 7).

When the liquid arrives in the contact with coating layer surface, the liquid front undergoes the wetting process of the constituent surfaces and the following bulk liquid fills first of all the smallest capillaries and finally proceeds into the large pores. This process is commonly explained by a purely hydrodynamic model [6,10,11], which assumes that the loss of energy during the liquid imbibition in the porous structure is based on the viscous drag within the spreading liquid. However, Schoelkopf et al. [38] draw attention to the role of pore size differentiating inertial effects, as summarised in the Bosanquet equation [23]. This differentiation means that the nanopores, if short, as they are in such coating structures, will constitute the first imbibing structure component by plug flow. Only later will the hydrodynamic viscous flow become active as a significant distance in the pore structure is filled and the larger reservoir pores also fill. At this latter stage, the balance between the wetting force of capillaries and the viscous drag determines the rate of progress. As the viscous drag increases in proportion to the length over which the liquid flows within the structure, and to the inverse of the fourth power of the typical equivalent capillary size (Poiseuille effect), there comes a point when the viscous drag equals the wetting force. If an external pressure is raised above the difference between the capillary force and the viscous drag, or when all the pores behind the wetting front are filled, then the action is by permeation flow according to Darcy's law in saturated structures. The bimodal behaviour of each curve illustrates the competition between the initial capillary wetting and the permeable flow characteristic once capillaries/pores behind the wetting front are filled.

It is interesting to note in Figs. 6A and C and 7B that the transition from the shorter time absorption to the longer time absorption for water in the presence of the 1 pph SA binder in MCC and PCC coatings shows a delay at the point of transition before the longer time behaviour is fully manifest. This suggests that there is a time controlling step required after the preferred pathway pores are filled, before the remaining structure can begin to fill. Such effects are either related to a change in structure or a diffusional effect, usually of surfactant origin [12,43]. Since the SA latex polymer matrix is known to be relatively inert to both oil and water, it is unlikely that structural changes are the cause for the delay. Rather, the surfactant associated with the latex may act as a wetting agent to allow passage of water via latex adjacent connecting throats in the pore network. The reorientation of the surfactant in relation to the wetting front may, therefore, control the access to the remaining pore network. Similar effects were seen by Ridgway et al. [42] in their study of the competitive absorption of hexadecane and water using dispersed GCC and similar SA latex as binder. Addition of further latex is likely to reduce permeability to such a level that the turning point of the slopes may disappear, as was seen by Ström et al. [43] with their 11 pph latex offset coatings.

Fig. 8 shows the results of short (upper figure) and long (lower figure) timescale absorption rates. At the short timescale, hexadecane absorbed quickest into the MCC coatings and the ground and precipitated calcium carbonate had very similar absorption rate values. However, the results for water were mostly on the same level in all tablets, only exception was the PCC based structure. The comparison between the short time results of binder containing MCC tablets shows that PVOH containing coatings absorbed water quicker than SA latex coatings. Fig. 7 shows that the results of long timescale absorption rates were smaller in ranking to those at short timescale. Both water and hexadecane absorbed quicker into the coating structures during the first 2 s time than after that. At

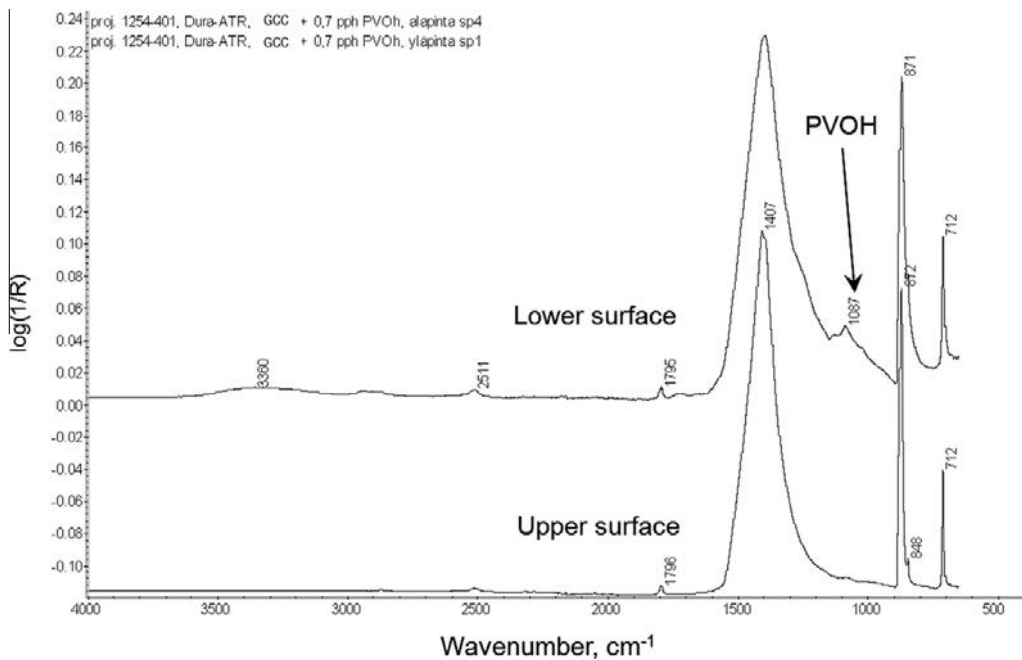


Fig. 2. The IR spectra of the tablet GCC with 0.7 pph PVOH (partially hydrolysed), measured with the FT-IR spectrometer. (Notice the lower PVOH content of colour in this measurement (=0.7 pph) compared with the actual tablets made for the microbalance measurement (1 pph). The lower surface was against the wire filter in the tablet former. The main peak of PVOH locates at the wavenumbers of 1087 cm^{-1} .

Table 3
Properties of water and hexadecane.

Liquid	Density (20 °C) (g cm^{-3})	Dielectric constant	Polarity index	Surface tension (mN m^{-1})	Viscosity (20 °C) (mPa s)
Water, H_2O	0.988	80.2	9.0^a , 10.2^b	72.8	1.002
Hexadecane, $\text{CH}_3(\text{CH}_2)_{14}\text{CH}_3$	0.773	2.0	0.0	27.5	3.340

^a Snyder [39].

^b Snyder [40].

Table 4
The thickness of binder films and the diffusion coefficient calculated with Eq. (4).

Binder film	Thickness (m)	Diffusion coefficient ($\text{m}^2\text{ s}^{-1}$)
PVOH (partially hydrolysed)	$2.25\text{E}-04$	$3.0\text{E}-13$
SA latex	$2.84\text{E}-04$	$3.5\text{E}-13$

long timescale, water provided higher absorption rates than hexadecane and the SA containing MCC coatings had now either the same or even higher absorption rate with water than the PVOH containing coatings.

3.3. Diffusion in binder films

The diffusion coefficient evaluation was made by studying the water vapour absorption into the binder films. The target of this small study was to find out the differences in the diffusion rate between the PVOH and SA latex films. In the real case of inkjet ink sorption, the aqueous-based ink diffuses quicker into the binder film than the vapour-form water because of the higher amount of water molecules, i.e. greater surface concentration of water. Fig. 9 shows how the studied PVOH film absorbs water to an amount of 37% of the film's original weight at 30 s, whereas in

the vapour-form the same film took up water to only 0.01 % under saturated humidity in addition to the amount already in the binder film under room temperature and humidity conditions. At the same time, the SA latex film absorbs a clearly lower amount of water or inkjet ink. Therefore, it can be assumed that during the inkjet ink setting process, the provided liquid water from the inkjet ink diffuses faster (concentration gradient dependent) into the binder film than the water moisture used in this part of the study. Additionally, the thickness of the polymer layer existing within nanopores will only constitute some few polymer molecules and so the path length for diffusion is also extremely short within such structure as the wetting front encounters the polymer.

There were two reasons why moisture rather than liquid water was selected to determine diffusion coefficient in this study. The first reason was that the absorption amount of SA binder film was low (Fig. 9) and the diffusion comparison between binder films needed to be made. The second reason was the accuracy of the crude immersion gravimetric method, where binder film was submerged into the water. Some of the polymer can transfer to the blotting boards, and in the case of hydrophilic PVOH film the polymer partially dissolves into the water during the measurement. Therefore, whilst the diffusion coefficient remains the same for moisture and for liquid water, the concentration difference is much

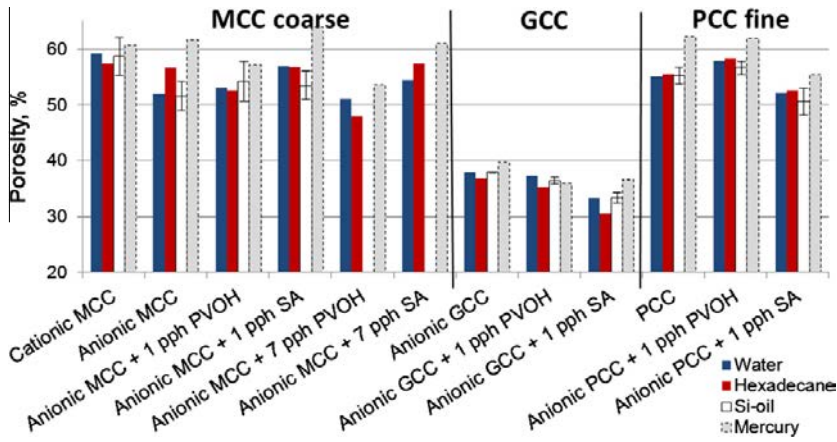


Fig. 3. The pore volume of coatings. Measured with Si-oil, water and hexadecane absorption and the mercury porosimetry.

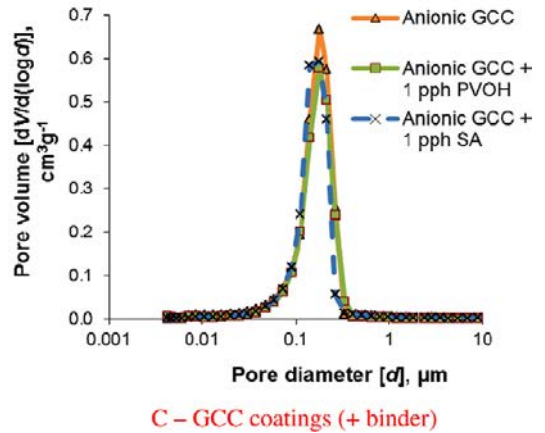
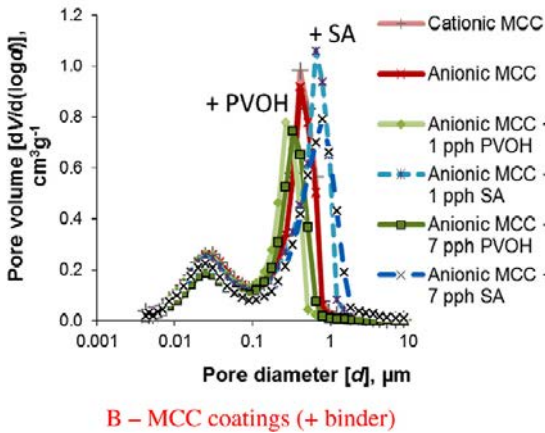
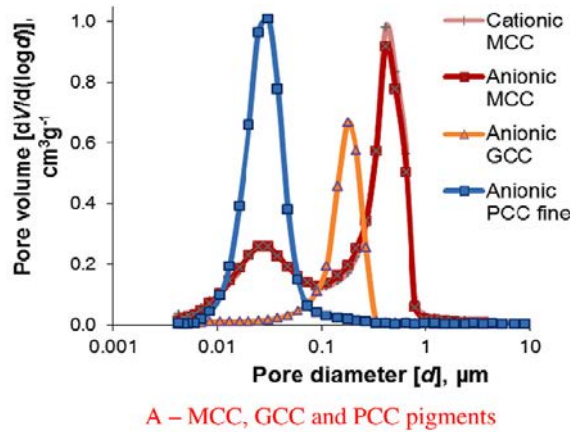


Fig. 4. The pore size distributions of the coating structures. (A) Differences between MCC, GCC and PCC pigment coatings (no binder addition). (B) The modified calcium carbonate (MCC) after adding the relevant binder amounts. (C) Ground calcium carbonate (GCC) as a function of a small amount of binder addition.

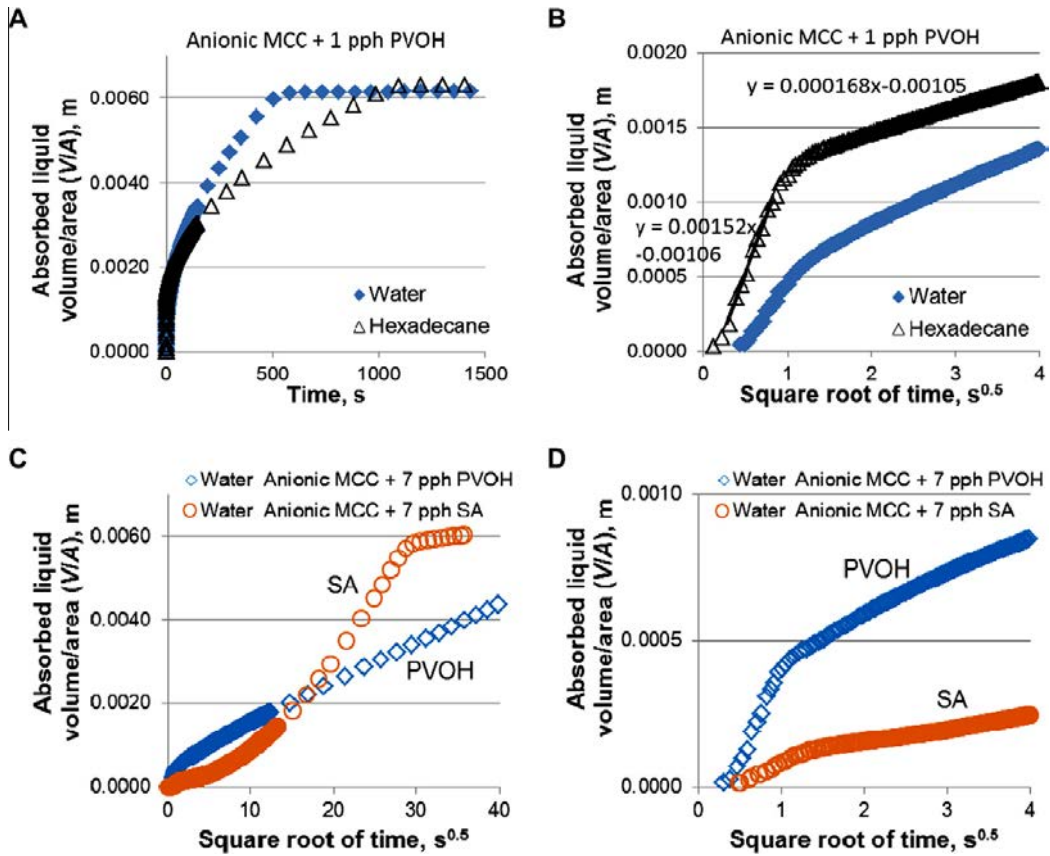


Fig. 5. The result curves of water and hexadecane imbibing into the anionic MCC coating structure with 1 pph PVOH (A and B). (A) Results of the measuring time up to 1500 s. (B) results of the first 4 s^{0.5}. (C) The result curves of water into the 7 pph PVOH and 7 pph SA latex containing coatings up to 40 s^{0.5}. (D) The same results as in C but the time scale is shorter, up to 4 s^{0.5}.

higher for liquid water at the polymer surface, and so the absolute uptake is greatly increased in the case of absorbing liquid.

Absorption data for water into binder films were analyzed using the techniques of Dynamic Vapour Sorption, DVS-1,¹⁴ which is a gravimetric moisture sorption measurement. The analyses were made with partially hydrolysed PVOH and SA latex films using different moisture contents of surrounding air. The results are shown in Fig. 10. The shape is that of an inverse exponential, and therefore we have applied the so-called Case II or Linear Driving Force Mass Transfer Model in the calculation of diffusion coefficient [44].

There was assumed to be an analogous substitution for heat transfer with mass transfer (thermal diffusivity “*a*” is replaced with moisture diffusion coefficient “*D*”), such that

$$\frac{M(\tau)}{M_{\text{Max}}} = 1 - \frac{4}{\pi} \sum_{n=0}^{\infty} \frac{(-1)^n}{(2n+1)} \times \cos\left(\frac{2n+1}{2}\pi\frac{x}{\delta}\right) \exp\left[-\left(\frac{2n+1}{2}\right)^2 \pi^2 \frac{D\tau}{\delta^2}\right] \quad (2)$$

where τ is time, D the molecular diffusion coefficient and n the consecutive layers. The other variables are described in Fig. 11. The Eq. (2) can be simplified for mass change of moisture in the middle of the plate, i.e. at $x = 0$ and for $n = 0$.

$$\frac{M(\tau)}{M_{\text{Max}}} = 1 - \frac{4}{\pi} \exp\left[-\frac{\pi^2 D\tau}{4\delta^2}\right] \quad (3)$$

In the Eq. (3) $4/\pi$ was taken away because at the initial time $\tau = 0$ the right side of the equation is negative, but it should be 0. So, following equation was used for diffusion coefficient estimation

$$\frac{M(\tau)}{M_{\text{Max}}} = 1 - \exp\left[-\frac{\pi^2 D\tau}{4\delta^2}\right] \quad (4)$$

The measured absorption amounts and the values from the diffusion Eq. (4) match very well (Fig. 12).

In this calculation, the diffusion was assumed to happen into the plate-like structure. This is actually valid for the PVOH and not for the latex. In the latex case, only a few water molecules can transfer into the film, meaning that the diffusion is more a surface diffusion. If we then decrease the thickness factor of the plate-like structure near zero, we shall get the surface diffusion. The mass transfer in the near-zero stage becomes zero in the Eq. (4), which cannot be true in the real liquid transfer. Nonetheless, the Eq. (4) fits the experimental diffusion data quite well. It delivers

¹⁴ Surface Measurement Systems, 5 Wharfside, Rosemont Road, Alperton, Middlesex, HA0 4PE.

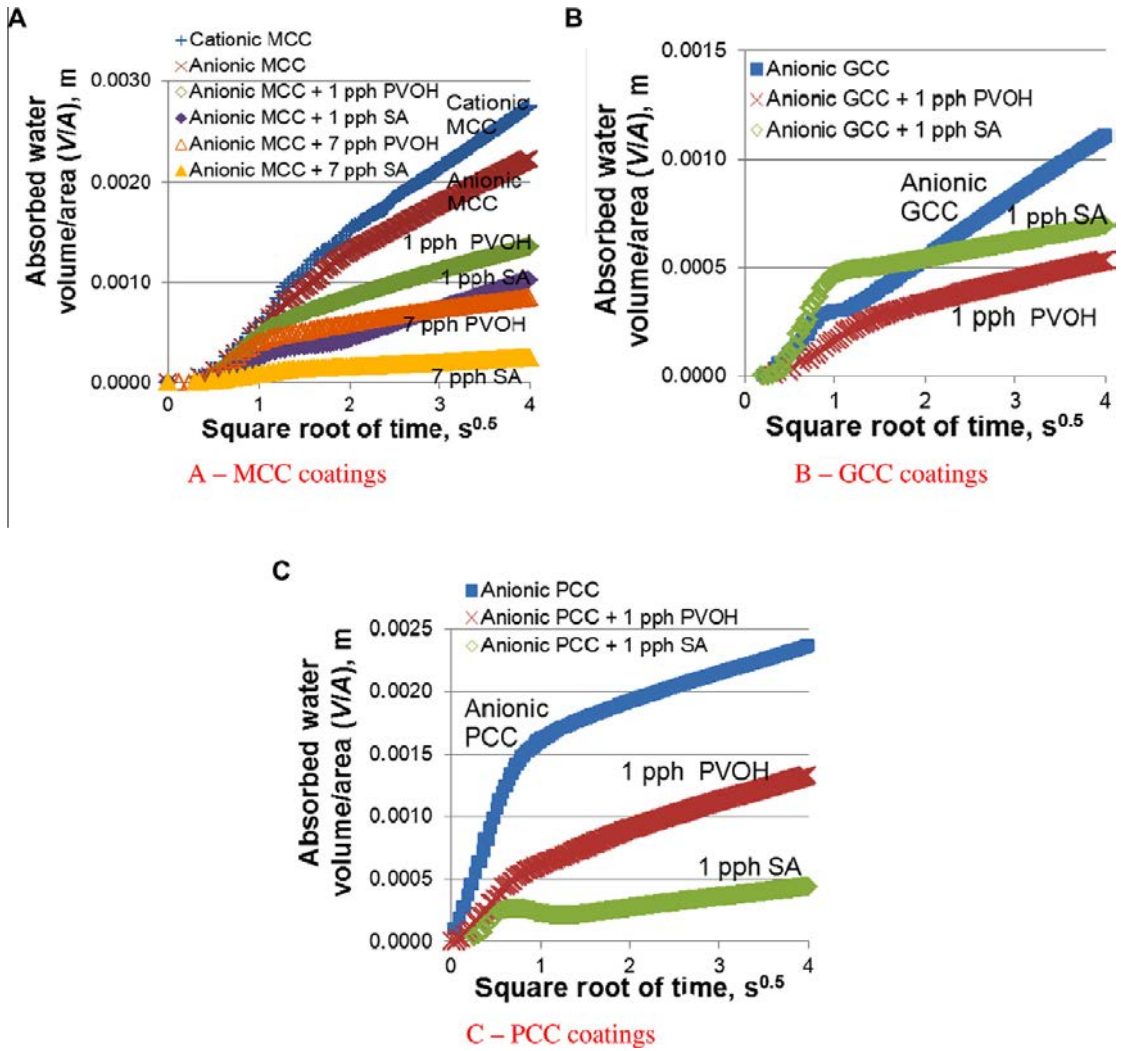


Fig. 6. Absorbed liquid volume/contact area of water (polar) and hexadecane (non-polar) into the studied coating structures. (A–C) The absorption amount of water into the MCC, GCC and PCC coatings, respectively.

a reasonable diffusion coefficient for latex, though it is insufficient for the latex case.

4. Discussion

Figs. 5–7 show that the results of absorbed liquid amount have two quite linear relations to the square root of time. This indicates either equilibrated Poiseuille laminar flow, only applicable to the long timescale [15,23] according a Lucas-Washburn-type equation, and/or a Fick’s Law diffusion response, which could apply to both the short as well as the long timescales. Fick’s first law describes the steady state of diffusion, where the concentration of diffusion volume is unchangeable during time. Fick’s second law describes the situation when the concentration within the diffusion volume changes during the time,

$$\frac{\partial c(x, t)}{\partial t} = D \frac{\partial^2 c(x, t)}{\partial x^2} \tag{5}$$

where $c(x, t)$ is the concentration of liquid at position x and time t . D is the diffusion constant. Thus, by dimensions, the denominator x^2 is proportional to the time t , and hence x is proportional to \sqrt{t} . Deriving from this, the diffusion length is often shown as $2\sqrt{(Dt)}$. The distance has a connection to the volume of liquid in the three-dimensional system and thus represents the mass of liquid uptake. Therefore, we can write the Eq. (5) as

$$\frac{m(t)}{t} = D \frac{A \cdot c(x, t)}{x} \tag{6}$$

where $m(t)/t$ is mass flow rate during the time t and area A of cross-section where the liquid is taken up.

4.1. Short timescale absorption

The short timescale absorption rate in Fig. 8 (upper side) shows that *non-polar* liquid (hexadecane) absorbs quicker in the anionic coating layer than polar liquid (water). The PCC coating without

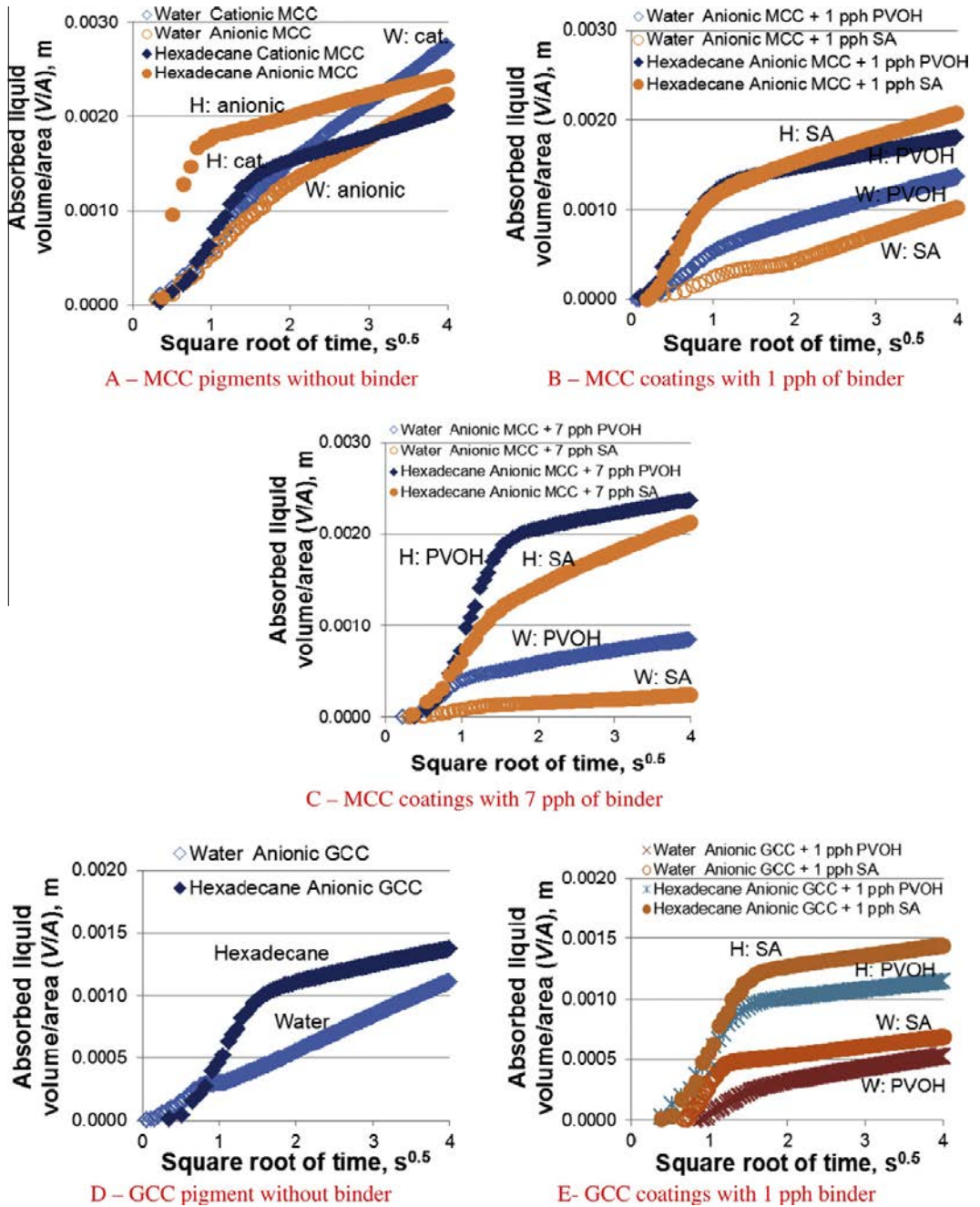


Fig. 7. (A–C) The differences between water and hexadecane absorption into the MCC coatings. (D and E) The absorption of water and hexadecane into the GCC pigment coatings. (H and J) The absorption of water and hexadecane into the PCC pigment coatings. In figures water has marked with abbreviation W and hexadecane with H.

binder forms the only exception, where water seems to absorb quicker than hexadecane in the structure. This was also shown by Ridgway and Gane [27]. One possible explanation also advanced by Ridgway et al. is that the chemical compounds used in the pigment dispersion may cause this difference. Both the GCC and the

MCC contain anionic polyacrylate dispersant, which itself requires a diffusion time for water to infiltrate the polymer network, swelling it and rendering it fully hydrophilic, whereas the PCC requires additional polyacrylate to render it more strongly anionic in dispersion. Thus, the PCC forms the notable exception in this series,

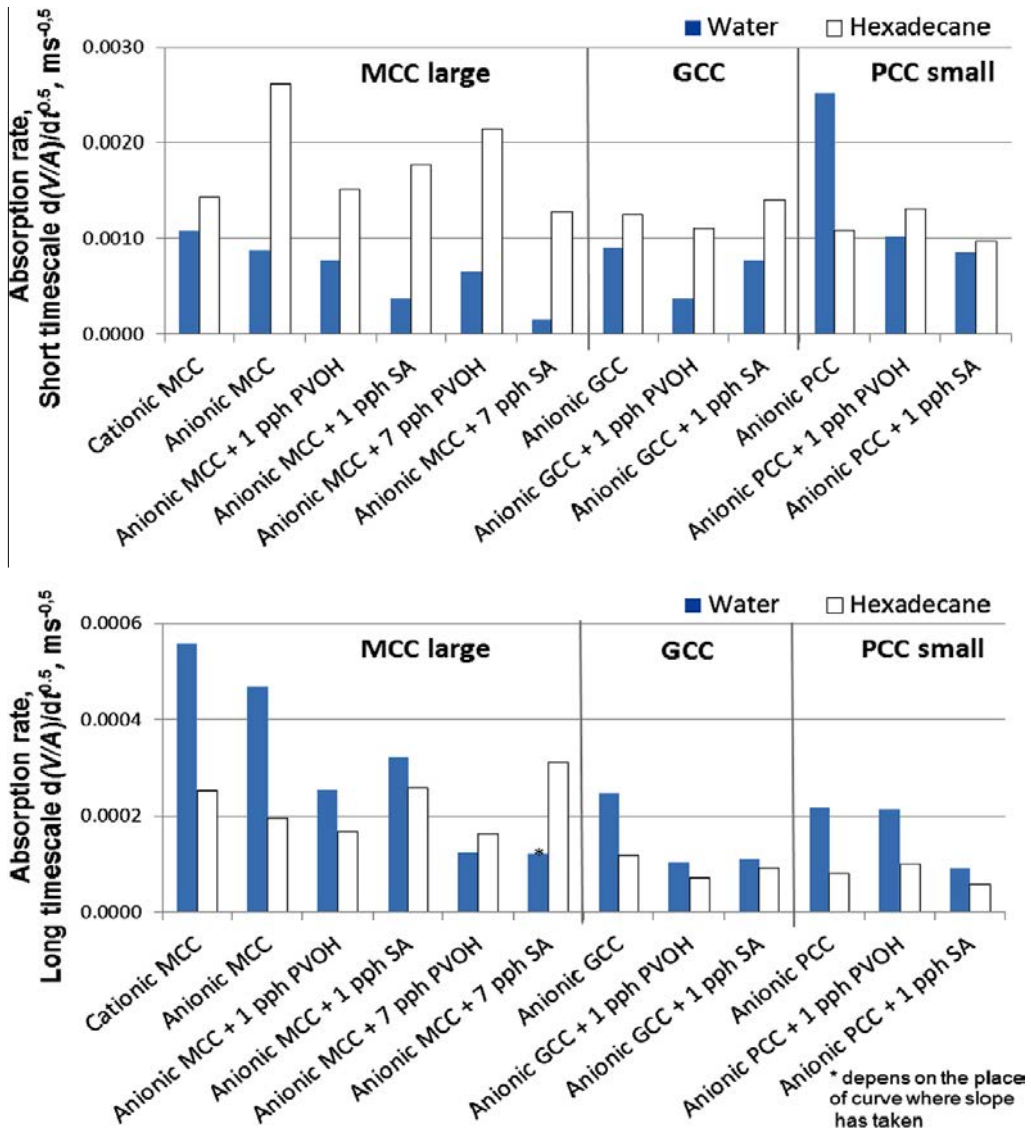


Fig. 8. Absorption rate of modified, ground and precipitated calcium carbonate pigment coatings. The short (upper figure) and long (lower figure) timescale $d(V(t)/A)/dt^{0.5}$ data are derived from the gradients of the curves, exemplified in Fig. 6, where the x-axis follows \sqrt{t} .

reversing the absorption preference from hexadecane to water at the shortest timescales.

The situation changes again when binder is present. The PVOH cannot absorb non-polar liquids meaning that swelling of the polymer in the presence of hexadecane is minimal. The smallest pores in the coating remain open during the hexadecane absorption and the diameters of inter-particle pores are unchanged [27]. Thus, during the non-polar liquid imbibition, the capillary flow dominates. In addition, the results show that the coating structure with both intra- and inter-particle pores (MCC) transports the hexadecane most effectively. Similar pore size structure coatings were found to be favourable for inkjet inks by Ridgway and Gane [27].

At short timescales, initially surprisingly, the slowest rate of absorption values with water were shown by the MCC/SA coatings, which had a slightly higher overall porosity and larger pores than the MCC/PVOH coating structures. The PVOH containing coating has more small pores than the SA coating. Thus, the apparent anomaly can be explained by the swelling of hydrophilic PVOH [28] changing the volume amount of small pores during the initial water absorption. The SA latex has a non-swelling nature [28,43] in the presence of water and thus the capillary flow controls the water imbibition in this case. The reason for slower absorption rate can be in the hydrophobic nature of SA latex that prevents the polar water penetration, probably related to the spatial orientation of surfactant and/or the carboxylation, used to stabilize the latex in

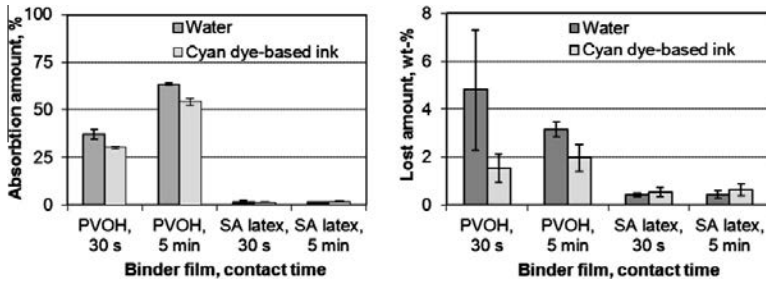


Fig. 9. Absorption of liquid water (A) into the PVOH and SA latex films (thickness about 200 μm) after 0.5 min and 5 min absorption time, and the loss of mass from the polymer film (B) into the water during the same measurement. The binder films were submerged into the water and removed after a certain time, dried gently between blotting boards and weighed.

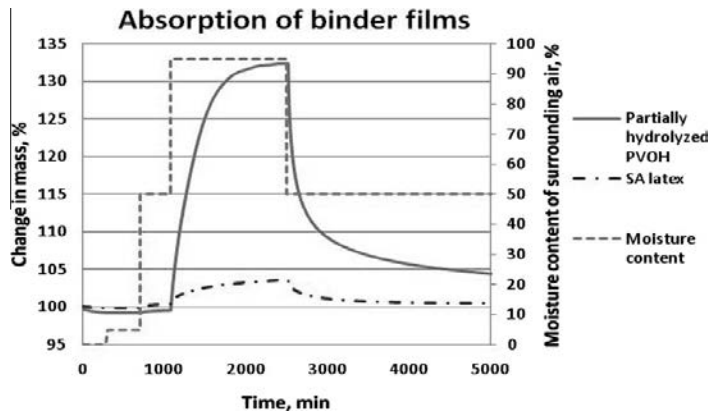


Fig. 10. Absorption curves for water vapour diffusion for different films.

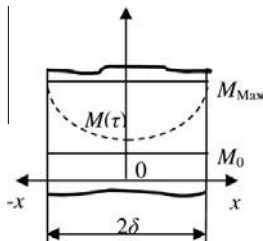


Fig. 11. A schematic view of the plate (film) body. M_0 is the initial moisture content in the plate; M_{Max} the maximum moisture content achievable in the plate.

dispersion, being both lower than in the case of anionically dispersed pigment and less polar than cationically dispersed systems. Similar binder behaviour in respect to water uptake was noticed with the PCC pigment coatings, too. It seems that the smallest pores are important in the polar liquid imbibition, but the necessary pre-diffusion into binder that inhabits these pores is an additional short timescale phenomenon. The capillary action controls the polar liquid imbibition in the short timescale, but the diffusion of water into binder polymer is also taking an active part in this process.

4.2. Long timescale absorption

In long time absorption (Fig. 8, lower side), the diffusion is still progressing but the porosity of the structure (permeation flow) permits the continued liquid imbibition by pore surface wetting and subsequent meniscus flow. In the long time area, the absorption rates are slower than in the short timescale area. In addition, the water absorbs quicker than hexadecane. The MCC coatings had again higher absorption rate values than either the GCC or the PCC containing coatings. The coating with the dual-porosity structure seems again to be the most advantageous.

When the MCC pigment with PVOH and SA containing coatings are compared on the long timescale, we can notice that the absorption rate of SA containing coating is the same or higher than that of the PVOH containing coating. In the over 2 s time absorption regime, the small diameter pores at the wetting front retain their action of providing the driving force, but the rate is determined by the permeation flow resistance to that driving force. These findings further support the conclusions of Ridgway and Gane [27].

4.3. Diffusion during inkjet ink absorption

The diffusion coefficients for water vapour in films made from the PVOH and SA latex binders are both close to $3 \cdot 10^{-13} \text{ m}^2 \text{ s}^{-1}$ (Table 4), whereas in the coating structures, such as the MCC pigment with 1 pph of PVOH or SA, they are each about $2.5 \cdot 10^{-11} \text{ m}^2 \text{ s}^{-1}$. In comparison, for cellulose fibres the water va-

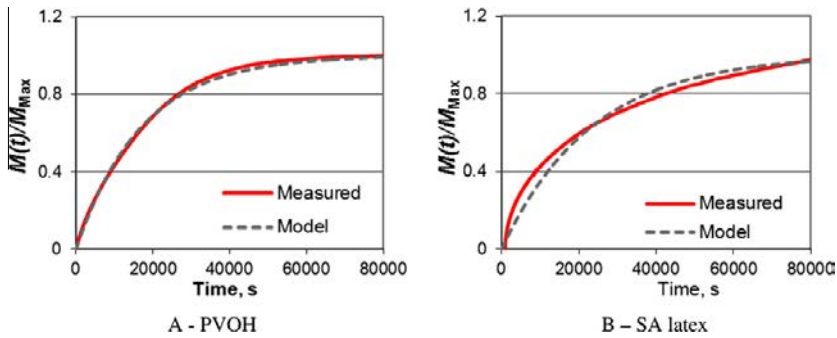


Fig. 12. The matching of model and measured data. (A and B) The measured absorption amounts divided by the maximum absorption of PVOH or SA latex films and the values of model (Eq. (4)), respectively.

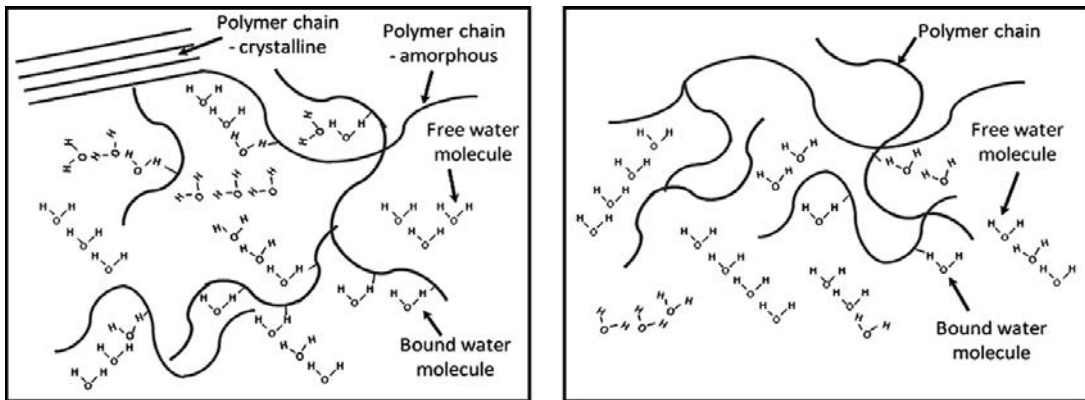


Fig. 13. The water molecules in the PVOH and SA latex polymer network.

pour diffusion coefficient is also about $10^{-11} \text{ m}^2 \text{ s}^{-1}$ [45], and for paper, with porosity of 20%, $10^{-8} \text{ m}^2 \text{ s}^{-1}$ [46]. Therefore, we can conclude that the permeability of the coating structure enhances the diffusion rate of that of binder alone. There are, then, no significant differences between the diffusion coefficient for PVOH and SA binder films or the coatings containing these binders. The same diffusion coefficient means that the flux of water vapour in these coatings is dominated by the pore structure of the coating, and thus also the local liquid concentration difference across the wetting front during the imbibition time. This supports the findings of Gane and Ridgway [34], who presented moisture pickup results from pigment tablets of dispersed GCC of various particle size distributions.

We suggest that, in the PVOH binder, the water molecules diffuse into the polymer chain network and form hydrogen bonds with the hydrophilic groups of the amorphous region of polymer whilst some of them remain as free water in the network. The water molecules cause the swelling of the binder and the further opening of the PVOH network microstructure so that the colourant molecules may subsequently fit into the binder structure (Fig. 13). In the SA latex case, the polymer microstructure has less chemical groups that could fix the water molecules and therefore there exists more free water than bound water in the network of SA binder during the water imbibition. The effective binding capacity of PVOH means that the polymer attracts (absorbs) the water molecules and the concentration of water in the PVOH is therefore higher than in the latex, although the diffusion rate of water vapour in relation

to the polymer itself remains similar. It seems that in the case of PVOH we identify possible “interpolymer” diffusion meaning that the diffusion is happening in the polymer network structure, whereas in the latex case the diffusion happens mainly on a surface of polymer network. It might be so that the surface properties of the latex extend for a significant distance from the actual surface, and we may suspect a swollen stabilizing layer. In the case of PVOH containing coating, the dominating diffusion can start from surface diffusion and osmosis, followed by Knudsen diffusion when the swelling has decreased the effective pore diameters. In the SA coatings, the role of Knudsen diffusion is assumed to be insignificant.

5. Conclusions

The results of the liquid uptake studies show that, in the beginning of the inkjet ink vehicle absorption, the small diameter (nano) pores play a dominant role and they provide the continuing driving force throughout imbibition. The capillary force drives the liquid into the coating structure. The polar liquid (water) diffuses into the polymer network of hydrophilic binder polymer (PVOH) and partially fixes there acting as a swelling agent, causing closure of some pores and a general diminishing of the binder-free portion and hence a reduction in pore diameters. This limits the available volume but assists the liquid faster absorption. The water molecule diffusion opens the PVOH polymer network. At the long timescale, the polymer swelling continues, but the permeation flow is the main

resistance determining factor to the capillary and surface diffusion controlled driving force in the continuing liquid mass transfer.

The absorption results of SA latex containing coatings show that the water uptake of initially hydrophobic coating proceeds more slowly at the short timescales, probably due to spatial orientation of latex stabilizing surfactant, whereas at the longer timescale the liquid transports quicker in the SA containing coatings than in the PVOH containing. It seems that the hydrophobic nature of latex prevents the diffusion of the polar liquid into the polymer network of the binder and there exists only a surface diffusion, probably related to the surfactant and/or carboxylation used to stabilize the latex.

References

- [1] H.R. Kang, *J. Imaging Sci.* 35 (3) (1991) 195–201.
- [2] M. von Bahr, F. Tiberg, B. Zhdud, *Langmuir* 15 (15) (1999) 7069–7075.
- [3] S.N. Reznik, A.L. Yarin, *Int. J. Multiphase Flow* 28 (9) (2002) 1437–1457.
- [4] A.U. Chen, O.A. Basaran, *Phys. Fluids* 14 (1) (2002) L1–L4.
- [5] O.A. Basaran, *AIChE J.* 48 (9) (2002) 1842–1848.
- [6] G. Desier, F. Deroover, F. De Voeght, A. Soucemanadin, *J. Imaging Sci. Technol.* 48 (5) (2004) 389–397.
- [7] F. Girard, P. Attané, V. Morin, *Tappi J.* 5 (12) (2006) 24–32.
- [8] J. Eggers, E. Villermaux, *Rep. Prog. Phys.* 71 (036601) (2008) 79.
- [9] A.N. Lembach, H.-B. Tan, I.V. Roisman, T. Gambaryan-Roisman, Y. Zhang, C. Tropea, L. Yarin, *Langmuir* 26 (12) (2010) 9516–9523.
- [10] N. Alleborn, H. Raszillier, *Chem. Eng. Sci.* 59 (10) (2004) 2071–2088.
- [11] C. Josserand, S. Zaleski, *Phys. Fluids* 15 (6) (2003) 1650–1657.
- [12] M. von Bahr, F. Tiberg, V. Yaminsky, *Coll. Surf. A: Phys. Chem. Eng. Aspects* 193 (1–3) (2001) 85–96.
- [13] J. Marmur, *Langmuir* 19 (14) (2003) 5956–5959.
- [14] R.A. Hayes, J. Ralston, *Langmuir* 10 (1) (1994) 340–342.
- [15] J. Schoelkopf, P.A.C. Gane, C.J. Ridgway, G.P. Matthews, *Colloid Surf. A* 206 (1–3) (2002) 445–454.
- [16] K.S. Sorbie, Y.Z. Wu, S.R. McDougall, *J. Colloid Interface Sci.* 174 (2) (1995) 289–301.
- [17] E.W. Washburn, *Phys. Rev.* 17 (3) (1921) 273–283.
- [18] J.M. Brethour, L.E. Scriven, in: *10th Int. Coating Sci. Tech. Symp.*, Scottsdale, USA, *Int. Soc. Coating Sci. Tech.*, 2000, pp. 97–100.
- [19] H. Gerung, Z. Yanrui, W. Li, R.K. Jain, T.J. Boyle, C.J. Brinker, S.M. Han, *Appl. Phys. Lett.* 89 (11) (2006) 111107 (p. 3).
- [20] H. Gerung, T.J. Boyle, L.J. Tribby, S.D. Bunge, C.J. Brinker, S.M. Tan, *J. Am. Chem. Soc.* 128 (15) (2006) 5244–5250.
- [21] J.S. Preston, N.J. Elton, A. Legrix, C. Nutbeam, J.C. Husband, *Tappi J.* 1 (3) (2002) 3–5.
- [22] C.J. Ridgway, P.A.C. Gane, *J. Colloid Interface Sci.* 252 (2) (2002) 373–382.
- [23] C.M. Bonsanquet, *Philos. Mag. Ser. 6*(45) (1923) 267, 525–531.
- [24] J. Kettle, T. Lamminmäki, P. Gane, *Surf. Coat. Technol.* 204 (12–13) (2010) 2103–2109.
- [25] R.J. Good, K.L. Mittal (Eds.), *Koninklijke Wöhrmann BV, Zutphen, The Netherlands*, 1993, pp. 3–36.
- [26] C.J. Ridgway, P.A.C. Gane, J. Schoelkopf, *Colloids Surf. A* 236 (1–3) (2004) J91–J102.
- [27] C.J. Ridgway, P.A.C. Gane, in: *TAPPI Coat. Conf.*, Toronto, Canada, Tappi Press, Atlanta, USA, 2005, 15pp.
- [28] T. Lamminmäki, J. Kettle, P. Puukko, P.A.C. Gane, C. Ridgway, in: *Int. Paper Coating Chem. Symp.*, Hamilton, Canada, 2009, 13p.
- [29] D.J. Shaw, *Introduction to Colloid & Surface Chemistry*, Reed Educational and Professional Publishing Ltd., 1996, 306p.
- [30] B. Liang, R.J. Fields, J.C. King, *Drying Technol.* 8 (4) (1990) 641–665.
- [31] H. Radhakrishnan, S.G. Chatterjee, B.V. Ramarao, *J. Pulp Pap. Sci.* 26 (4) (2000) 140–144.
- [32] A.T. Ahlen, *Tappi J.* 53 (7) (1970) 1320–1326.
- [33] G. Desie, G. Deroover, F. De Voeght, A. Soucemanadin, *J. Imaging Sci. Technol.* 48 (5) (2004) 389–397.
- [34] P.A.C. Gane, C.J. Ridgway, in: *TAPPI 10th Adv. Coating Fund. Symp.*, Montreal, Canada, Tappi Press, Atlanta, USA, 2008, 24p.
- [35] R. Eriksson, J. Merta, J.B. Rosenholm, *J. Colloid Interface Sci.* 326 (2) (2008) 396–402.
- [36] P.A.C. Gane, G.P. Matthews, J. Schoelkopf, C.J. Ridgway, D.G. Spielmann, in: *TAPPI Adv. Coating Fund. Symp.*, Toronto, Canada, Tappi Press, Atlanta, USA, 1999, pp. 213–236.
- [37] C.J. Ridgway, P.A.C. Gane, *Nordic Pulp Pap. Res. J.* 17 (2) (2002) 119–129.
- [38] J. Schoelkopf, P.A.C. Gane, C.J. Ridgway, J. Spielmann, G.P. Matthews, *Tappi J.* 2 (6) (2003) 9–13.
- [39] L.R. Snyder, *J. Chromatogr. A* 92 (2) (1974) 223–230.
- [40] L.R. Snyder, J.L. Glajch, J.J. Kirkland, *Practical HPLC Method Development*, second ed., Wiley, New York, NY, USA, 1988, pp. 722–723.
- [41] P.A. Gane, J.P. Kettle, G.P. Matthews, C.J. Ridgway, *Ind. Eng. Chem. Res.* 35 (5) (1996) 1753–1764.
- [42] C.J. Ridgway, J. Schoelkopf, P.A.C. Gane, in: *Tappi Adv. Coating Fund. Symp.*, Munich, Germany, Tappi Press, Atlanta, GA, USA, 2010, 19p.
- [43] G.R. Ström, J. Borg, E. Svanholm, in: *TAPPI 10th Adv. Coating Fund. Symp.*, Montreal, Canada, Tappi Press, Atlanta, USA, 2008, pp. 204–216.
- [44] H.S. Carslaw, *Conduction of Heat in Solids*, Clarendon Press, Oxford, UK, 1997, p. 100.
- [45] D. Topgaard, O. Söderman, *Langmuir* 17 (9) (2001) 2694–2702.
- [46] E.K.O. Hellen, J.A. Ketoja, K.J. Niskanen, M.J. Alava, *J. Pulp Pap. Sci.* 28 (2) (2002) 55–62.